ISSN 1845–8319

KINEMATICS OF UMBRAL FINE STRUCTURE

M. SOBOTKA[1], K. G. PUSCHMANN[2], and H. HAMEDIVAFA[3]

[1] *Astronomical Institute AS CR, CZ-25165 Ondřejov, Czech Republic*
[2] *Instituto de Astrofísica de Canarias, E-38205 La Laguna, Spain*
[3] *Physics Department, Imam Khomeini International University, 34149-16818 Qazvin, Iran*

Abstract. A 2-hour long series of white-light images of a large sunspot acquired in June 2004 with the 1-m Swedish Solar Telescope at La Palma is utilized to study the evolution and motions of small-scale umbral structures – umbral dots and features in faint light bridges. For this purpose, a newly improved feature-tracking code is applied. The small-scale structures move with average speeds of 0.34 km s^{-1} either into the umbra or along the faint light bridges. Structures that do not split or merge are smaller (0.″15) than the average size (0.″17). Brightness and size variations of individual non-split/merge structures are positively correlated during their evolution.

Key words: Sunspots - umbra

1. Introduction

Sunspot umbrae show a variety of small-scale bright structures embedded in a dark umbral background: umbral dots (UDs, Danielson, 1964), light bridges (LBs) with a rich internal structure, and extensions of bright penumbral filaments. In time series of high-resolution images, these structures are observed to move horizontally and undergo a complex evolution, changing their brightness and size, splitting into two or more features or merging with other ones. For a review see e.g. Sobotka (2003).

In this paper we continue the work about the behaviour of UDs and fine features in faint LBs inside a large dark umbra (Sobotka and Puschmann, 2007, hereafter Paper I), presenting preliminary results about the kinematics, evolution, and size distribution of these structures. The knowledge of these characteristics may provide observational constraints to theoretical models of sunspots.

2. Observations and Data Processing

The leading sunspot of NOAA 10634, located near disk centre, was observed on 18 June 2004 from 07:43 to 15:30 UT with the 1-m Swedish Solar Telescope (SST, Scharmer et al., 2003), equipped with adaptive optics. The images were acquired in a frame-selection mode (selection interval 20 s), simultaneously in three wavelength bands: blue (4507.5 ± 4.6) Å, red (6020.0 ± 13.0) Å, and G-band (4308.6 ± 5.8) Å. Exposure times were 11–14 ms and the pixel size was $0\farcs0405$. The red band with the best signal-to-noise ratio (200) was selected for the further analysis. The images were corrected for stray light (6.5 %) and deconvolved for the instrumental profile of the telescope. The spatial resolution was estimated to $0\farcs14$. The frames were aligned, destretched, and a subsonic filter (cutoff 4 km s^{-1}) was applied to the time series. We selected the best part of the series from 12:15 to 14:12 UT, containing 350 frames, with the field of view $20\farcs25 \times 20\farcs25$. The observations and data reduction are described in detail in Paper I.

The central part of the umbra is dominated by two extremely weak LBs, composed of small aligned point-like features. Bright peripheral UDs move into the umbra. Central UDs are often clustered and create granule-like structures (see Paper I). To improve the visualization and feature tracking, we suppressed large-scale intensity variations in the umbra. A smooth intensity "background" was calculated for each frame, using 2D spline fits to local intensity minima in the umbra, and averaged over a period of 140 s (7 frames). This interpolated time-variable "background" intensity was subtracted from the images.

The motions of umbral features were studied using the methods of local correlation tracking (LCT, November and Simon, 1988) and feature tracking (Sobotka et al., 1997). The feature tracking procedure was recently updated by Hamedivafa (2008). A substantial improvement was made in image segmentation (separation of bright features from the background), where a new low-noise curvature determination algorithm was used. The feature-tracking technique was also improved, so that now it is possible to distinguish features that passed split or merge events from those that were not influenced by these events. Newly, a split/merge event breaks the history of a feature. This approach prevents ambiguous tracking of features, but, on the other hand, it introduces a spurious shortening of lifetimes.

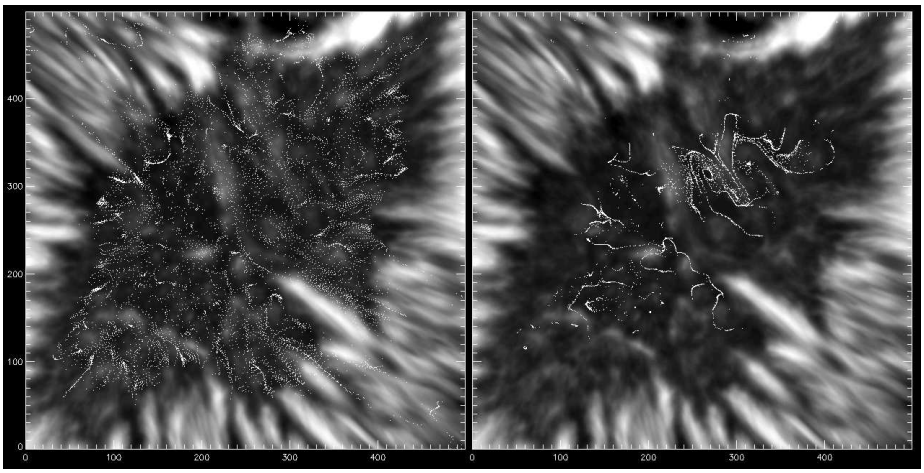

Figure 1: Two snapshots of the 24-min cork movie, at 4 min *(left)* and 20 min *(right)*. The cork positions are calculated using a velocity map derived by LCT. Underlying grey-scale images are averages of the whole time series. The field of view is $20\farcs25 \times 20\farcs25$.

3. Results

LCT provides a time-averaged horizontal velocity field of all structures in the field of view. The FWHM of the Gaussian tracking window was set to $0\farcs32$ and the temporal integration was made over 60 min and 117 min (full length of the series). There is no substantial difference between the velocity fields obtained with different integration times. The results can be visualized either using a velocity map (published in Paper I) or by means of a cork movie. The latter method (Molowny-Horas and Yi, 1994) utilizes hypothetical particles, "corks", carried by the calculated velocity field. The positions of corks were sampled every 12 s and after 24 min most of the corks finished in stable positions. Two snapshots of the cork movie are shown in Fig. 1.

At the beginning of the cork movie (Fig. 1 left), the corks at the periphery of the umbra align into paths directed toward the umbral centre. This means that peripheral UDs move inwards, following some preferred trajectories. These trajectories are influenced by local brightness inhomogeneities inside the umbra. Near the end of the movie (Fig. 1 right), the corks are already swept out from the periphery of the umbra by the inward-directed

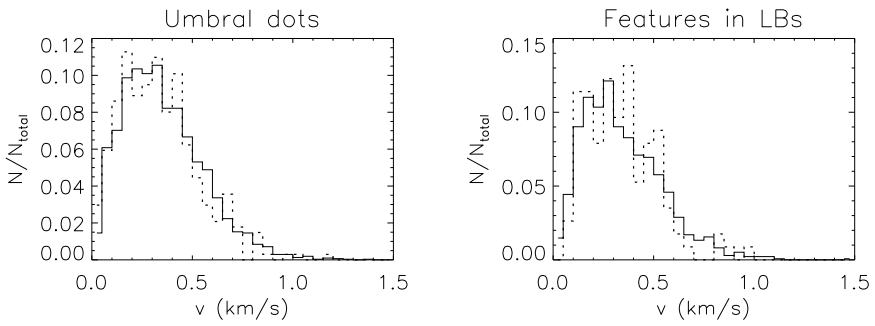

Figure 2: Histograms of time-averaged horizontal velocity magnitudes, derived from feature tracking. Dotted line – non-split/merge structures, solid line – all structures.

velocity field. They concentrate in thread-like structures that depict places with convergent, shear, or zero motions. For example, a dark nucleus (zero motions) on the upper left side of the umbra is partially outlined by these threads. The elliptic cork pattern located to the right of the dark nucleus is formed by a complex velocity shear between two faint LBs, where motions of bright features along each bridge have opposite directions.

The feature tracking procedure provides instantaneous positions, horizontal velocities, intensities, sizes, and corresponding average values for each individual feature. We selected 3099 UDs and 1357 bright features in LBs for the futher study, using the following criteria: The object must be brighter by 4 % (of the mean intensity of quiet granulation) than the surrounding umbra, its area must be larger than 9 pixels (corresponding to effective diameter of $0\farcs137$ or 100 km), it must live longer than 2 min, and must not move faster than 3 km s^{-1}.

Of 3099 UDs, only 337 did not split or merge during their evolution. Similarly, of 1357 bright features in LBs, 114 were unaffected by split or merge. We see that splitting and merging of small-scale structures are very frequent in the umbra. There are at least three mechanisms for that. The first one is the variable seeing. Two or more nearby structures, resolved in good-quality images, may merge into one unresolved structure when the seeing deteriorates and again split when it improves. These spurious split/merge events can be avoided using efficient image-restoration methods or in case of space observations. The second mechanism is a positional

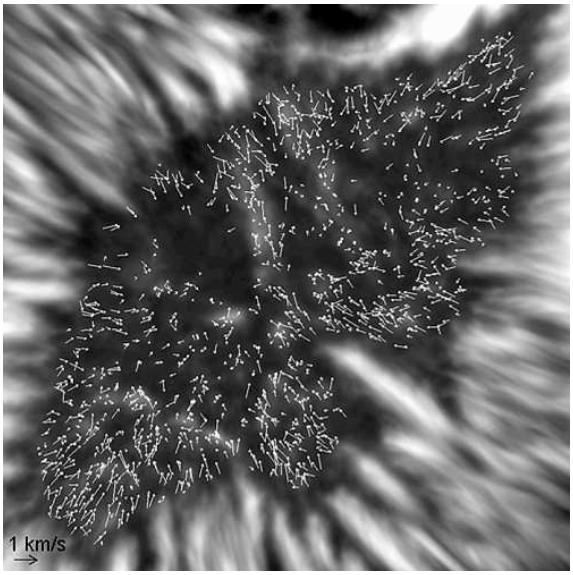

Figure 3: Time-averaged horizontal velocity vectors of UDs and bright features in LBs living longer than 5 min, derived from feature tracking. The field of view is $20\farcs25 \times 20\farcs25$.

coincidence of two different structures, e.g. one moving and one stationary, also observed in our time series. The third possibility is a real "physical" split or merge process.

Time-averaged horizontal velocities were calculated separately for UDs and bright features in LBs. Histograms of velocity magnitudes are plotted in Fig. 2, where non-split/merge structures are depicted by dotted lines and all structures with solid ones. All histograms are similar, with mean values around 0.34 km s^{-1}. The asymmetry of the velocity distribution points to two possible populations: slow (< 0.4 km s^{-1}) and fast (> 0.4 km s^{-1}). Vectors of time-averaged horizontal velocities are shown in Fig. 3 for 1401 structures with lifetimes longer than 5 min. We see that inward-oriented motions dominate in the umbra. The spatial distributions of slow and fast populations generally overlap but fast structures are missing in the central parts of the umbra and no structures with lifetimes longer than 5 min are detected in the dark nucleus, where the strongest magnetic field is expected.

Observed sizes of small-scale structures are an important constraint

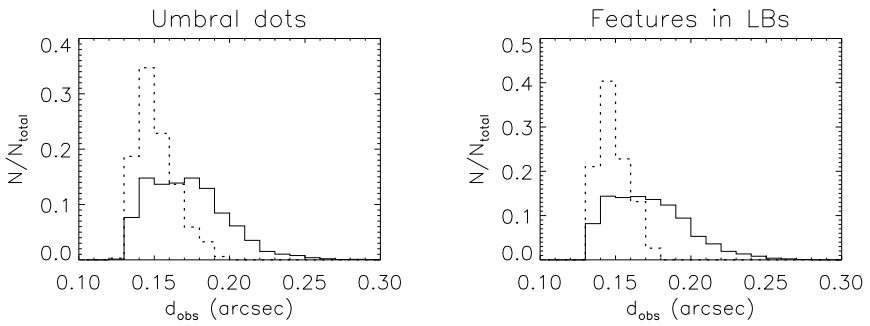

Figure 4: Histograms of time-averaged effective diameters, derived from feature tracking. Dotted line – non-split/merge structures, solid line – all structures.

for theoretical models. Histograms of effective diameters calculated from time-averaged areas of all 3099 UDs and 1357 bright features in LBs (solid lines) and of 337 UDs and 114 bright features in LBs that did not split or merge (dotted lines) are plotted in Fig. 4. It can be seen that UDs and bright features in LBs do not differ in size. However, the non-split/merge structures have narrower range of sizes and smaller mean size ($0\farcs15$) than all structures in the sample (with the mean size of $0\farcs17$). Larger diameters of splitting or merging structures suggest that these structures may be composed of small unresolved objects.

The time-averaged values of brightness, size, and horizontal velocity of small-scale structures in the umbra are completely uncorrelated. However, during the evolution of an individual structure, there is a correlation between the brightness excess ΔI (with respect to the surrounding umbra) and the area of the structure. An example of evolution of a long-lived central UD is shown in Fig. 5 (left). Coefficients of correlation between ΔI and area evolution were calculated for the non-split/merge structures (337 UDs and 114 bright features in LBs) and the histograms are plotted in Fig. 5 (right). The brightness and size temporal variations are positively correlated in most cases – 50 % of features have correlation coefficients higher than 0.48 and the typical value of correlation is 0.60. The structures first grow and brighten and then get smaller and fainter, in agreement with theoretical predictions (Schüssler and Vögler, 2006).

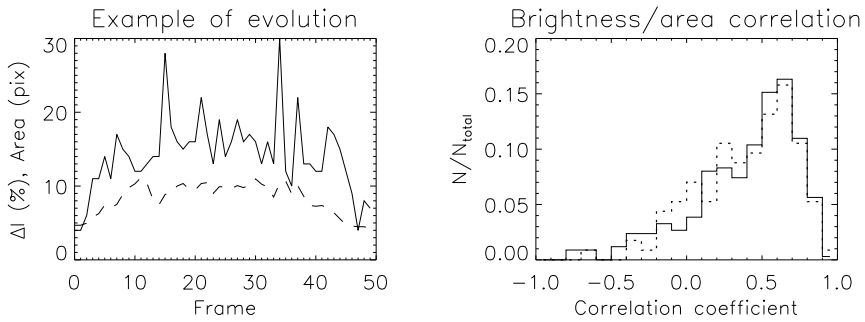

Figure 5: *Left:* An example of area (solid) and brightness (dashed) evolution of a central UD. *Right:* Histograms of correlation between brightness and area during the evolution of individual structures. Solid line – UDs, dotted line– bright features in LBs.

4. Conclusions

We analyze an excellent 2-hour long series of broadband images (6020.0 ± 13.0 Å) of a large sunspot NOAA 10634, acquired on 18 June 2004 with the 1-m Swedish Solar Telescope at La Palma. The preliminary results of the study of umbral small-scale structures and their kinematics can be summarized as follows:

The majority (90 %) of observed structures split or merge with other structures. This can be a real physical effect, but in many cases it is due to seeing variations or random spatial coincidences.

Motions of umbral bright structures are directed either into the umbra or along faint LBs. In the central parts of the umbra, the motions are influenced by local brightness inhomogeneities, where we expect different strengths of magnetic field.

Time-averaged velocity magnitudes (0.34 km s^{-1} on average) are similar for UDs and bright features in LBs and do not depend on split or merge of the structures. Structures faster than 0.4 km s^{-1} appear mostly at the periphery of the umbra and in faint LBs, where the magnetic field is weaker and more inclined.

Non-split/merge structures are clearly smaller (0.″15) than the average size (0.″17) of all structures. This means that structures showing the split or merge events may be composed of small unresolved objects.

Although the time-averaged values of brightness, size, and horizontal velocity of structures are uncorrelated, during the evolution of individual non-split/merge features, temporal brightness variations are positively correlated with size variations in most cases.

Acknowledgements

We thank C. Möstl, R. Kever, and R. Henderson for assisting the observations. This work was supported by the grant IAA 3003404 of the Grant Agency of the Academy of Sciences of the Czech Republic (AS CR), by the Research Plan AVOZ 10030501 of AS CR, by the OPTICON Transnational Access Programme, and by the Spanish Ministerio de Educación y Ciencia through the project ESP 2006-13030-C06-01. The SST is operated by the Royal Swedish Academy of Sciences in the Spanish Observatorio del Roque de los Muchachos of the Instituto de Astrofísica de Canarias.

References

Danielson, R.: 1964, *Astrophys. J.* **139**, 45.

Hamedivafa, H.: 2008, *Solar Phys.*, submitted.

Molowny-Horas, R. and Yi, Z.: 1994, Internal Report No. 31, Institute of Theoretical Astrophysics, University of Oslo.

November, L. J. and Simon, G. W.: 1988, *Astrophys. J.* **333**, 427.

Scharmer, G. B., Bjelksjö, K., Korhonen, T. K., Lindberg, B., and Petterson, B.: 2003, in S. Keil & S. Avakyan (eds.), *Innovative Telescopes and Instrumentation for Solar Astrophysics*, Proc. SPIE, **4853**, 341.

Schüssler, M. and Vögler, A.: 2006, *Astrophys. J.* **641**, L73.

Sobotka, M.: 2003, *Astron. Nachr.* **324**, 369.

Sobotka, M., Brandt, P. N., and Simon, G. W.: 1997, *Astron. Astrophys.* **328**, 682.

Sobotka, M. and Puschmann, K. G.: 2007, in F. Kneer, K. G. Puschmann, and A. D. Wittmann (eds.), *Modern Solar Facilities – Advanced Solar Science*, Universitätsverlag Göttingen, 205.